Available online at www.sciencedirect.com
SCIENCE DIRECT®
Journal of Solid State Chemistry 179 (2006) 538–543
JOURNAL OF SOLID STATE CHEMISTRY
www.elsevier.com/locate/jssc

Synthesis and characterization of molybdenum carbides using propane as carbon source

Xiao-Hui Wang, Hong-Ling Hao, Ming-Hui Zhang*, Wei Li, Ke-Yi Tao

Institute of New Catalytic Materials Science, College of Chemistry, Nankai University, Tianjin 300071, PR China

Received 7 September 2005; received in revised form 30 October 2005; accepted 9 November 2005
Available online 13 December 2005

Abstract

Bulk face-centered-cubic (fcc)-based η-MoC_{1-x} and hexagonal-close-packed (hcp)-based β-Mo_2C have been prepared using C_3H_8/H_2 by temperature-programmed reaction method and a rapid heating method. In this work, direct carburization of MoO_3 produces η-MoC_{1-x} or MoO_xC_y with excess carbon, different from that with CH_4/H_2 or C_2H_6/H_2 as carburization reagent. A successive post-treatment by hydrogen causes the phase transformation from fcc-based η-MoC_{1-x} or MoO_xC_y to hcp-based β-Mo_2C. Amorphous SiO_2-supported β-Mo_2C is also successfully prepared by the two methods and passes through the same route as the bulk one. HRTEM, BET surface area measurements and thiophene hydrodesulfurization reaction are conducted for the comparison of the two methods. The results indicate that different ramping rates bring slight difference in specific surface area and initial catalytic activity but obvious difference in particle size to the final product supported β-Mo_2C.

Keywords: Molybdenum carbide; Temperature-programmed reaction; Rapid heating; Post-treatment; Phase transformation; Thiophene; Hydrodesulfurization

1. Introduction

Transition metal carbides, a kind of solid-state materials with some outstanding properties in mechanical hardness, thermal stability, and especially in catalytic performance, have been extensively studied over the past three decades [1–6]. Groups VI transition metal carbides are proved to be excellent active species in hydrogen transfer reactions [7–10], methane reforming [11], ammonia synthesis [12], etc., and their catalytic properties are usually superior to the noble metal catalysts in selectivity, stability and resistance to poison [13]. Thus, they are considered as potential substitutes for noble metal-based catalysts.

The conventional method for the preparation of carbide catalysts utilizes the temperature-programmed reactions (TPRe), in which gas hydrocarbons as well as carbon monoxide [14,15] are used as carbon sources flowing over various precursors at a slow heating rate (0.5–5 K min^{-1}). The precursors herein usually include metals, metal oxides and metal nitrides. As supplements to gas state carbon sources, liquid state and solid state sources [16–24] have also been developed based on TPRe method or other routes such as carbothermal reduction and alkalide reduction method. To our knowledge, the carburizing reagent has great effects on final carbides in preparation conditions, formation process, surface area as well as particle size and morphology. Traditionally, CH_4/H_2 [3,25–28] and C_2H_6/H_2 [29–31] are the most widely utilized mixtures in the preparation of molybdenum-based carbides with TPRe method, direct carburization of which leads to phase pure β-Mo_2C [29,31]. And it is proved that C_2H_6/H_2 can lower the required synthesis temperature and the size of the resultant products comparing with CH_4/H_2. As the non-routine carbon source, C_4H_8/H_2 [32,33] and C_2H_2/H_2 [5] have been established to be potential agents for the preparation of molybdenum carbides at lower temperature. Their advantage should be owing to the high carbon content and the early production of atomic carbon. In this respect, the analogical property and superiority of propane

*Corresponding author. Fax: +86 22 23507730.
E-mail address: zhangmh@nankai.edu.cn (M.-H. Zhang).

0022-4596/$ - see front matter © 2005 Elsevier Inc. All rights reserved.
doi:10.1016/j.jssc.2005.11.009

may be expected. However, limited attention has been paid to the carburizing with propane, except that Mo–W sulphide [34] and Mo metal are used as precursors [15].

It is well demonstrated that the details of the TPRe method conditions used for the synthesis procedure are critical to obtaining high surface area product that is potentially useful as a catalyst. Several studies have been done to investigate the relationship between the heating rate and the microstructure properties of the resultant bulk carbides, whereas almost all of researchers altered the ramping rate in a narrow range [8,35,36]. Choi et al. reported that increasing ramping rate from 1 to 2 K min^{-1} could increase the specific surface area of molybdenum carbides [8]. However, varying the ramping rate in the same manner on vanadium carbide decreased the specific surface area to some extent [35]. In addition, Kwon et al. proposed that varying the heating rate within the range from 1 to 3 K min^{-1} did not significantly affect the properties of the vanadium carbides, which differed from the above results [36]. In short, it is hard to reach an acknowledged conclusion about the effect of ramping rate on bulk materials in previous studies. On the other hand, investigation of ramping rate on supported materials is blank up to now.

In this work, the bulk and amorphous SiO_2-supported molybdenum carbides were prepared by carburization reagent C_3H_8/H_2 with TPRe method; the synthesis process was investigated and a post-treatment by hydrogen was revealed to be necessary for the preparation of β-Mo_2C. Moreover, a rapid heating method was developed and determined to be effective to prepare molybdenum carbides, in particular for the supported samples. Since supported β-Mo_2C showed good activities in many reactions, thiophene hydrodesulfurization (HDS) was used as model reaction and studied over as-prepared supported catalysts at various temperatures, providing more direct evidences for the comparison between the rapid heating method and TPRe method.

2. Experimental section

MoO_3, the precursor of bulk samples, was prepared by calcining ammonium heptamolybdate ($(NH_4)_6Mo_7O_{24}\cdot 4H_2O$, analytical grade) at 773 K for 5 h. The powder was pressed under 20.0 MPa to obtain 40–60 mesh particles and then placed in a 10-mm (o.d.) silica tube plugged with silica wool at both ends for successive process. Carburizing reagent was C_3H_8/H_2 with the fixed molar ratio 1:5 and the volume hourly space velocity (VHSV) of the flowing mixture was 6000 h^{-1}. In the series of experiments, the ramping rate was operated in two ways. For the TPRe method, the ramping rate was 10 K min^{-1} from room temperature to 623 K and 1 K min^{-1} from 623 K to the final temperature 923 K; for the rapid heating method, 10 K min^{-1} was employed from room temperature to 923 K. The holding time for both methods at the final temperature was 1.5 h. In order to discriminate the samples prepared by two different methods, TPR and RH was used to denote the samples. In addition, for some of the experiments, a post-treatment was carried out at the final temperature by switching the carburization reagent to pure hydrogen or argon for another 1.5 h. For example, the sample denoted as TPR-H_2 means it was prepared by TPRe method and a post-treatment by hydrogen was adopted subsequently before cooling. All the samples were cooled to room temperature in hydrogen flow and passivated in a 1% (v/v) O_2/N_2 gas flow for 3 h.

The preparation of amorphous SiO_2-supported carbides with 20.2 wt% Mo loading rates was similar to that of the bulk samples described previously. The oxide precursor was prepared by mixing finely grounded SiO_2 and aqueous solution of $(NH_4)_6Mo_7O_{24}\cdot 4H_2O$ followed by drying and calcination in air. The carburization process was performed as above, except that the time of the post-treatment was extended by 1 h.

X-ray diffraction (XRD) patterns of the passivated samples were acquired on a Rigaku D/max-2500 powder diffractometer employing Cu$K\alpha$ source. Scanning electron microscopy (SEM) images were obtained using a Hitachi S-3500N scanning electron microscope. A JEM-2010FEF high-resolution transmission electron microscope (HRTEM) equipped with an EDX system (EDAX) operating at 200 kV was conducted to observe the morphology and microstructure of the samples. The molybdenum analyses of the samples were carried out with an IRIS advantage inductively coupled plasma atomic emission spectrometer (ICP-AES), and the carbon contents of the samples were determined using an Elementar Vario EL elemental analyzer. BET surface areas of the supported samples were determined from N_2 BET isotherms by Automatic Surface Area and Pore Size Analyzer (Autosorb-1-MP 1530VP) apparatus.

Thiophene HDS activity measurements were carried out in a pulse microreactor applying H_2 as carrier. The SiO_2-supported catalysts prepared by above two methods were evaluated at the temperature ranging from 553 to 653 K after reduced by hydrogen. Thiophene HDS activities were calculated in units of nanomoles of thiophene converted to products per gram of catalyst per second (nmol Th/g cat/s).

3. Results

3.1. The bulk molybdenum carbides

A series of molybdenum carbides were prepared with the carburization reagent C_3H_8/H_2. As shown in Fig. 1, the products obtained by the two methods are similar in the location and intensity of the peaks. The diffraction peaks of sample TPR and sample RH are weak, and three dispersion peaks appear at 37°, 62° and 74°, which can be assigned to characteristic peaks of the metastable η-MoC_{1-x} [33] or molybdenum oxycarbide [32] with a face-centered cubic (fcc) arrangement of molybdenum

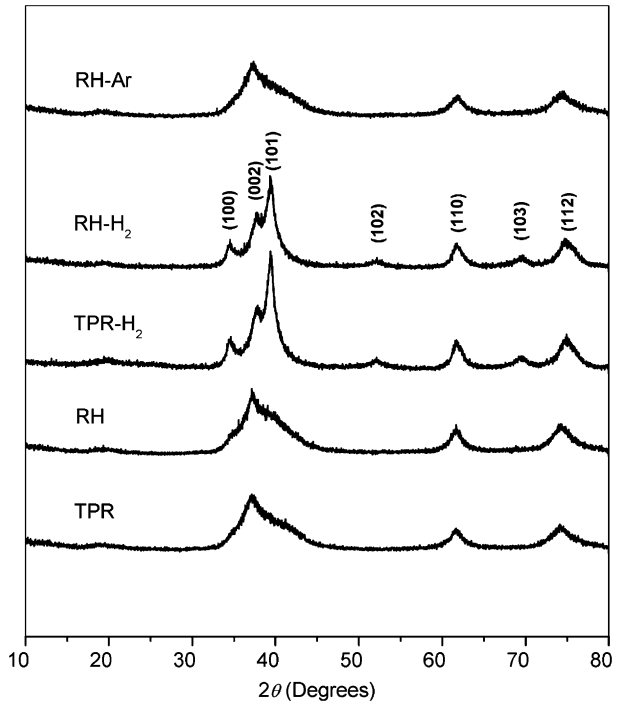

Fig. 1. XRD patterns of the bulk samples.

Table 1
Chemical composition and average crystallite sizes of the samples

Sample	Chemical composition	Average crystallite size (nm)[a]
RH	$MoC_{1.05}$	6.2
RH-H_2	$Mo_2C_{0.98}$	7.2
RH-Ar	$MoC_{1.04}$	6.4

[a]Derived from XRD patterns and calculated with the Scherrer equation.

atoms, as discussed later. According to the data listed in Table 1, the atomic ratio C/Mo of the sample RH is 1.05. And the existence of the excess carbon is confirmed. This is supported by the observation of HRTEM, through which free carbon can be clearly observed. From the viewpoint of XRD, the resultant products are independent of ramping rate through it varies in a board range. Besides, if the carburization time was extended for another 1.5 h, no obvious change could be observed in crystal structure and carbon content.

As shown in Fig. 1, the fcc-based carbide was transformed into hcp-based carbide β-Mo_2C ($P63/mmc$) after post-treated by pure hydrogen at the final temperature 923 K, with all the diffraction peaks identical with the crystallographic planes (card no. 35-0787) [37]. Samples TPR-H_2 and RH-H_2 present almost the same appearances. To make clear the function of hydrogen, argon was introduced to the post-treatment. However, the XRD pattern of the sample RH-Ar remains unchanged in comparison with the precursor sample RH. Table 1 gives the elemental composition along with the average crystallite sizes of the samples prepared by the rapid heating method. After post-treated by argon, almost no changes occur, as listed in Table 1. That is to say, argon cannot bring about phase transformation and hydrogen takes part in the transformation process.

The SEM images of the samples TPR, RH, TPR-H_2 and RH-H_2 are given in Fig. 2. The morphology of their parent orthorhombic MoO_3 has the platelet structure [32,38]. After carburization, this original morphology does not exist any more. In Fig. 2, sample TPR appears as relatively regular particles with the size of 1–3 μm, and sample RH presents irregular star-like particles varying from 3 to 7 μm in diameter. The uniform phase of sample TPR can be attributed to the relatively mild course of increasing the temperature. As shown in Fig. 2 TPR-H_2 and RH-H_2, the morphologies of them have changed in comparison with their precursors. It is interesting to find that the two samples are similar to each other in shapes, present as irregular platelets accumulating together layer by layer.

3.2. The amorphous SiO_2-supported molybdenum carbides

With the metal loading 20.2 wt%, the characteristic peaks of β-Mo_2C in Fig. 3 are noticeable for supported samples prepared by both methods. As Fig. 3 shows, the same intermediate η-MoC_{1-x} is observed for bulk and supported samples carburized by C_3H_8/H_2. With respect to the preparation process, the time of the post-treatment with pure hydrogen was lasted for 2.5 h, which was essential for the complete phase transformation and established by the experimental experience. Comparing with the bulk ones, the supported samples needed one more hour for post-treatment, which should be tentatively attributed to the strong interaction between the metal and the support. At the same time, the ramping rate also has few influences on the specific surface areas of the SiO_2-supported samples, which are 166.1 $m^2 g^{-1}$ for sample TPR-H_2/SiO_2 and 170.7 $m^2 g^{-1}$ for sample RH-H_2/SiO_2.

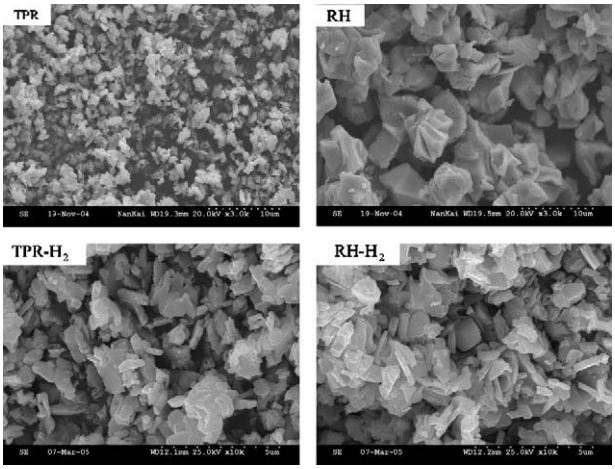

Fig. 2. SEM images of the bulk samples.

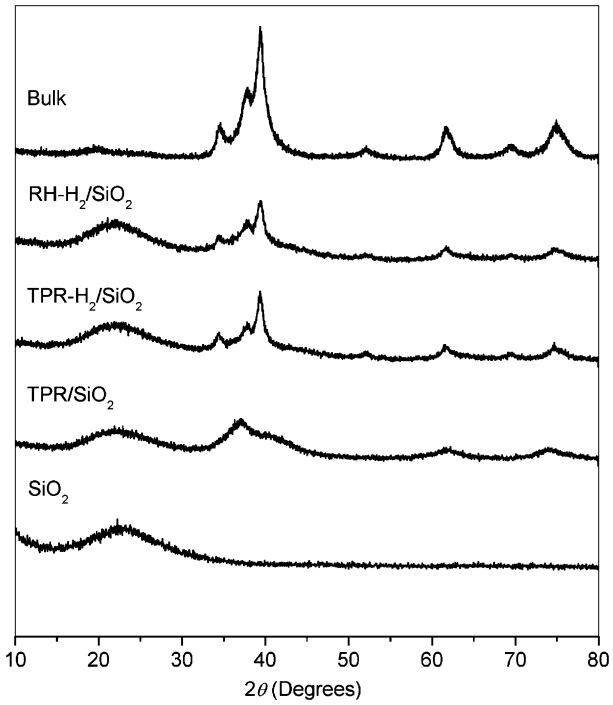

Fig. 3. SiO_2-supported carbides prepared by the two methods.

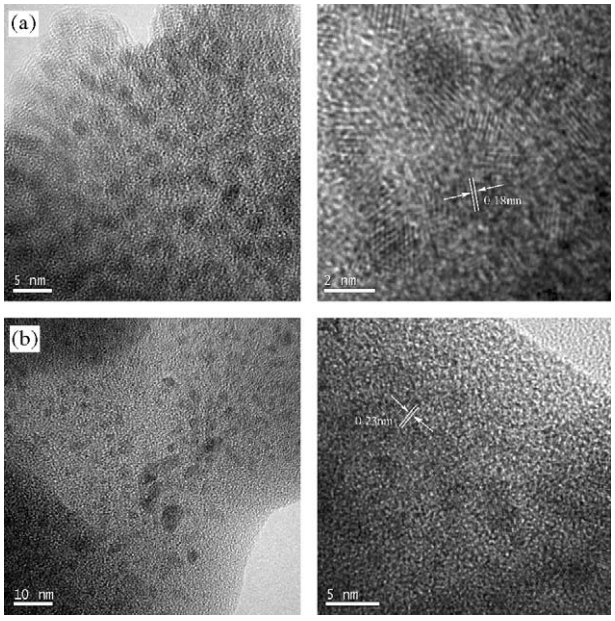

Fig. 4. HRTEM micrographs of SiO_2-supported β-Mo_2C: (a) sample TPR-H_2/SiO_2; and (b) sample RH-H_2/SiO_2.

Shown in Fig. 4 are the bright field HRTEM micrographs of the supported β-Mo_2C samples. Observation of Fig. 4a shows fairly uniform particles with the size of ca. 2.5 nm display an excellent dispersion on the support. In the case of Fig. 4b, the carbides particles distributing over the support possesses sizes in the range of 2–5 nm. The difference in size between Fig. 4a and b should be ascribed

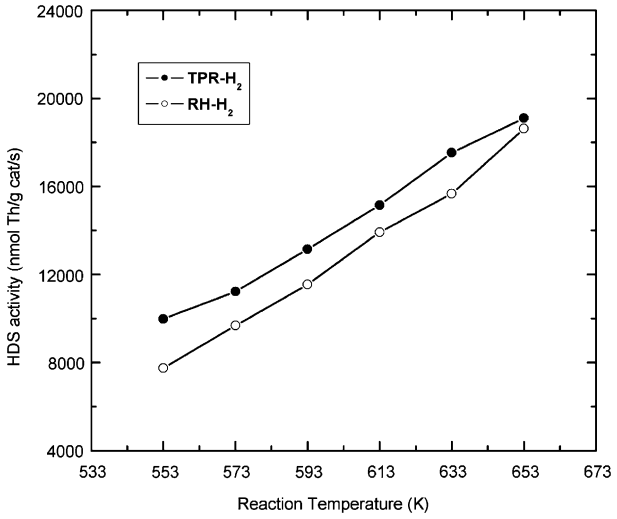

Fig. 5. Thiophene HDS activities for SiO_2-supported β-Mo_2C as a function of the reaction temperature.

to the original differences between the samples before post-treatment in morphology. This has also been proposed by the inspection of SEM images of bulk samples. Furthermore, the HRTEM micrographs of sample TPR-H_2/SiO_2 and RH-H_2/SiO_2 yield d-spacing values of 0.18 and 0.23 nm for the (102) and (101) crystallographic planes, respectively, which are in good agreement with the XRD results. Catalytic activities of amorphous SiO_2-supported β-Mo_2C samples were measured for HDS of thiophene to testify the efficiency of the above synthesis route and further access the effect of the ramping rates on the catalytic properties. The results were plotted in Fig. 5. Both samples showed high initial HDS catalytic activities. And it can be concluded that the activity of the sample TPR-H_2/SiO_2 is slightly higher than RH-H_2/SiO_2, which may reflect the dispersion state of the active species and is consistent with the HRTEM measurements.

4. Discussion

4.1. The synthesis process

The conventional method to prepare the active species β-Mo_2C is utilizing the temperature-programmed reaction at the final temperature above 973 K with the carburization reagent CH_4/H_2. Propane used as carbon source by far has been seldom reported in the previous researches, in particularly oxide used as precursor. In our study, the synthesis process passes through an intermediate MoC_{1-x} or molybdenum oxycarbide to obtain β-Mo_2C under the experimental conditions employed, resembling the route of C_4H_{10} being used as carbon source [32]. Thus, comparing the performance of light gas hydrocarbon such as CH_4 and C_2H_4 in preparing molybdenum carbides, propane and butane used as carbon source shows analogical property, which is proposed below.

It is well known that C_3H_8 and C_4H_{10} decompose at lower temperature relative to CH_4 and C_2H_6. Reliable conclusion has been drawn in literatures [29,31,33], in which CH_4, C_2H_6 and sometimes C_4H_{10} were brought into comparison. In the synthesis process, the carbon source C_3H_8 decomposed and active atomic carbon which can insert into the lattice of the molybdenum oxide generated. When atomic carbon was produced in the early stage at relatively lower temperature, initial carburizing took place. At the same time, small molecular hydrocarbon deposited over the surface of the samples that could have been turned into polymeric carbon with the hydrogen content diminishing. As shown in Fig. 6, the pyrolytic carbon layer formed the onion-like structure [21], and the inserted EDX result revealed that only carbon could be detected in this microregion. Thus, excess carbon was proved to be present in the intermediate, which accorded with the data listed in Table 1. The absence of crystalline carbon phases in the XRD patterns indicated the deposited carbon was amorphous. However, because of the great excess of the carburizing mixture, the carbon yielded from pyrogenation covered the surface of the intermediate, which was perhaps a barrier to further carburizing and accounted for the incomplete replacement of oxygen by carbon. That is maybe the reason why the process of C_3H_8 and C_4H_{10} using as carbon source pass through the same route to phase pure β-Mo_2C. The research on carburization reagent C_4H_{10} made by Xiao et al. [32] coincides with this deduction, in which similar intermediate was obtained by TPRe method at 923 K, and the existence of H_2O and carbon oxide determined by TPRe-MS in the temperature range from 923 to 1023 K reflects the presence of oxygen in the intermediate.

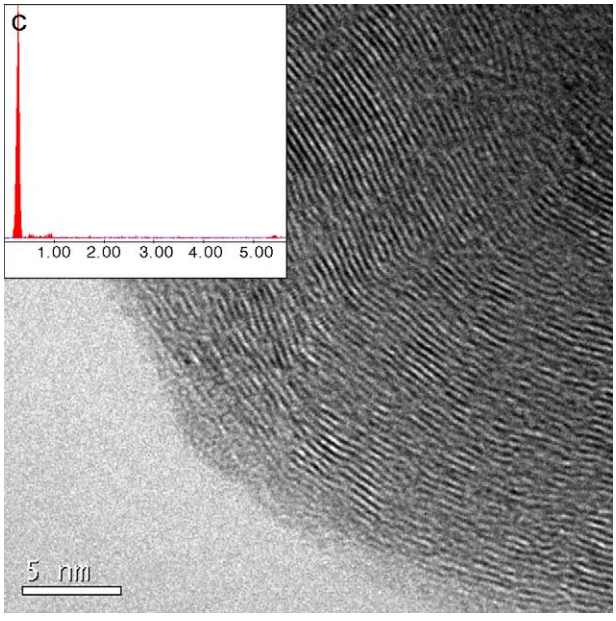

Fig. 6. HRTEM micrograph of the sample RH. The inset is the EDX result of this microregion.

The post-treatment by hydrogen at the final temperature could cause the transformation from fcc oxycarbide to hcp carbide. In order to confirm what kind of role hydrogen played in this step, inert gas argon replaced hydrogen to define if thermal effect was the dominating factor in the phase change. However, excess carbon was still contained in the species and no phase transformation could be observed. The results above allow us to presume the function of hydrogen and the transformation process as follows. At the final temperature 923 K, deposited polymeric carbon could be converted into gas hydrocarbon by hydrogenation, which made it possible for oxygen atoms in the bulk to escape from the crystal lattice in the form of H_2O. If the flow was still consisted of C_3H_8 and H_2, the deposition of amorphous carbon derived from C_3H_8 and the hydrogenation of polymeric carbon was simultaneous. Therefore, it is reasonable to conclude that C_3H_8 plays little further role in the phase transformation process.

4.2. Effects of the ramping rates

As have been investigated in previous study, for the molybdenum carbide prepared from the molybdenum trioxide, the resultant high surface area mainly generated in the initial section of MoO_3 being reduced to form MoO_2 or MoO_xC_y $(x+y<1)$ [31]. Namely, when the precursor is treated in a slow and linear manner, the cracking and degradation of the platelet-like smooth MoO_3 crystal occurs gently. Such a procedure may expose more structure defects, produce an increased porosity and lead to higher surface area carbides. It was also emphasized the heating rate played an important role in the conversion of the molybdenum phases in the crystallographic motif.

Generally, catalyst with high surface area and small particle size is desired to have improved catalytic activity, which can usually be acquired by optimizing experimental conditions. However, the study of Choi et al. did not support this established rule any more, which revealed the activity of Mo_2C for the hydrogenation of benzene, expressed per unit of surface, increased with the increasing particle size and decreasing surface area of the Mo_2C crystallites [39]. Taking all of these into consideration, the rapid heating method is developed for the preparation of carbide catalyst in this paper and compared with the TPRe method.

As noted above, the preparation of phase pure β-Mo_2C with the two methods undergoes similar conversion of molybdenum phases. Since the transformation of molybdenum oxycarbide to β-Mo_2C took place at the fixed final temperature without the influence of heating rate, it is concluded that the ramping rate is of less importance in our synthesis route on crystallographic motif as well as surface area, porosity and particle size of the final products. More evidence can be found in the SEM images. Before H_2 post-treatment, the particle of sample RH is several times greater than that of sample TPR; after, they are almost of the same morphologies and sizes. This may be due to the

removing the oxygen in the crystal lattice, which leads to a lattice mismatch and structural rebuilding in the phase transformation.

With respect to application of β-Mo_2C to catalysis, amorphous SiO_2-supported samples are synthesized through the TPRe and rapid heating method. It is well known that support is often utilized to promote better distribution of catalyst, which can greatly increase the surface area of the catalyst. In our study, the little differences in specific surface area between the two supported samples indicate the similar distribution for the active species on the support. More information for comparison is provided by HRTEM measurements, through which the effects of ramping rate on particle size of the active species is intuitionistic and distinct. That is, the TPRe method leads to a fairly uniform distribution for the metal component and the rapid heating method results in a distribution slightly inferior to the former. In addition, the catalytic performance of the samples is examined to focus on the distribution of the active species on the support; the initial activities of the samples prepared through two routes are close to each other, which is identified with the results of HRTEM measurements.

5. Conclusion

Bulk and supported fcc η-MoC_{1-x} or MoO_xC_y and hcp β-Mo_2C were synthesized using C_3H_8/H_2 as carbon source. β-Mo_2C was prepared through a post-treatment by hydrogen, in which step propane could play little further role. A rapid heating method was proved to be as effective as conventional TPRe method for the preparation of molybdenum carbides. The removing of oxygen by hydrogen in the phase change from fcc-based carbide to hcp-based carbide led to a lattice mismatch and structural rebuilding, which weakened the effects of ramping rates that worked on the crystallographic motif of the final products. The dispersion of the active species on the support prepared by two methods reflects the effects of the ramping rates. HRTEM measurements and initial catalytic activities in thiophene HDS reaction provided similar evidence for the comparison.

Acknowledgments

The authors thank for the financial support of the National Natural Science Foundation of China (Grants 20403009), the Key Project of Chinese Ministry of Education (No. 105045), and Open Foundation of State Key Laboratory of Heavy Oil Processing.

References

[1] S.T. Oyama, The Chemistry of Transition Metal Carbides and Nitrides, Blackie Academic, London, 1996.
[2] J.H. Sinfelt, D.J.C. Yates, Nat. Phys. Sci. 229 (1971) 27–28.
[3] J.S. Lee, S.T. Oyama, M. Boudart, J. Catal. 106 (1987) 125–133.
[4] S.T. Oyama, Catal. Today 15 (1992) 179–200.
[5] T. Xiao, H. Wang, J. Da, K.S. Coleman, M.L.H. Green, J. Catal. 211 (2002) 183–191.
[6] J.G. Chen, Chem. Rev. 96 (1996) 1477–1498.
[7] L. Delannoy, J.M. Giraudon, P. Granger, L. Leclercq, G. Leclercq, Catal. Today 59 (2000) 231–240.
[8] J.-G. Choi, J.R. Brener, L.T. Thompson, J. Catal. 154 (1995) 33–40.
[9] A.P.E. York, J.B. Claridge, J. Brungs, S.C. Tsang, M.L.H. Green, Chem. Commun. 1 (1997) 39–40.
[10] M.K. Neylon, S. Choi, H. Kwon, K.E. Curry, L.T. Thompson, Appl. Catal. A 183 (1999) 253–263.
[11] M.L. Pritchard, R.L. McCauley, B.N. Gallaher, W.J. Thomson, Appl. Catal. A 275 (2004) 213–220.
[12] R. Kojima, K.-I. Aika, Appl. Catal. A 219 (2001) 141–147.
[13] M.J. Ledoux, C. Pham-Huu, H. Dunlop, J. Guille, J. Catal. 134 (1992) 383–398.
[14] P.N. Ross, P. Stonehart, J. Catal. 48 (1977) 42–59.
[15] M. Saito, R.B. Anderson, J. Catal. 63 (1980) 438–446.
[16] S.T. Oyama, P. Delporte, C. Pham-Huu, M.J. Ledoux, Chem. Lett. 26 (1997) 949–950.
[17] Y. Li, Y. Fan, G. Luo, Ind. Eng. Chem. Res. 43 (2004) 1334–1339.
[18] J.A. Nelson, M.J. Wagner, Chem. Mater. 14 (2002) 4460–4463.
[19] J.A. Nelson, M.J. Wagner, Chem. Mater. 14 (2002) 1639–1642.
[20] C. Liang, W. Ma, Z. Feng, C. Li, Carbon 41 (2003) 1833–1839.
[21] B. Bokhonov, Y. Borisova, M. Korchagin, Carbon 42 (2004) 2067–2071.
[22] C. Liang, P. Ying, C. Li, Chem. Mater. 14 (2002) 3148–3151.
[23] C. Liang, F. Tian, Z. Li, Z. Feng, Z. Wei, C. Li, Chem. Mater. 15 (2003) 4846–4853.
[24] Y. Shin, X.S. Li, C. Wang, J.R. Coleman, G.J. Exarhos, Adv. Mater. 16 (2004) 1212–1215.
[25] L. Volpe, M. Boudart, J. Solid State Chem. 59 (1985) 348–356.
[26] J.S. Lee, L. Volpe, F.H. Ribeiro, M. Bourdart, J. Catal. 112 (1988) 44–53.
[27] J.C. Schlatter, S.T. Oyama, J.E. Metcalfe III, J.M. Lambert Jr., Ind. Eng. Chem. Res 27 (1988) 1648–1653.
[28] R. Kapoor, S.T. Oyama, J. Solid State Chem. 155 (2000) 320–326.
[29] J.B. Claridge, A.P.E. York, A.J. Brungs, M.L.H. Green, Chem. Mater. 12 (2000) 132–142.
[30] T.C. Xiao, A.P.E. York, H. Al-Megren, C.V. Williams, H.T. Wang, M.L.H. Green, J. Catal. 202 (2001) 100–109.
[31] A. Hanif., T.C. Xiao, A.P.E. York, J. Sloan, M.L.H. Green, Chem. Mater. 14 (2002) 1009–1015.
[32] T.-C. Xiao, A.P.E. York, V.C. Williams, H. Al-Megren, A. Hanif, X.-Y. Zhou, M.L.H. Green, Chem. Mater. 12 (2000) 3896–3905.
[33] T.-C. Xiao, A.P.E. York, K.S. Coleman, J.B. Claridge, J. Sloan, J. Charnock, M.L.H. Green, J. Mater. Chem. 11 (2001) 3094–3098.
[34] T.H. Nguyen, E.M.T. Yue, Y.J. Lee, A. Khodakov, A.A. Adesina, M.P. Brungs, Catal. Commun. 4 (2003) 353–359.
[35] J.-G. Choi, J. Catal. 182 (1999) 104–116.
[36] H. Kwon, L.T. Thompson, J. Eng Jr., J.G. Chen, J. Catal. 190 (2000) 60–68.
[37] JCPDS Powder Diffraction File, International Centre for Diffraction Date, Swarthmore, PA, 2000.
[38] K.T. Jung, W.B. Kim, C.H. Rhee, J.S. Lee, Chem. Mater. 16 (2004) 307–314.
[39] J.-S. Choi, G. Bugli, G. Djega-Maradassou, J. Catal. 193 (2000) 238–247.